Spectral Tuning of Avian Violet- and Ultraviolet-Sensitive Visual Pigments

Susan E. Wilkie,[‡] Phyllis R. Robinson,[§] Thomas W. Cronin,[§] Subathra Poopalasundaram,[‡] James K. Bowmaker,[||] and David M. Hunt*,[‡]

Departments of Molecular Genetics and Visual Science, Institute of Ophthalmology, University College London, Bath Street, London, EC1V 9EL, U.K., and Department of Biological Sciences, University of Maryland Baltimore County, 1000 Hilltop Circle, Baltimore, Maryland 21250

Received December 3, 1999; Revised Manuscript Received April 12, 2000

ABSTRACT: The violet- and ultraviolet-sensitive visual pigments of birds belong to the same class of pigments as the violet-sensitive (so-called blue) pigments of mammals. However, unlike the pigments from mammals and other vertebrate taxa which, depending on species, have λ_{max} values of either around 430 nm or around 370 nm, avian pigments are found with λ_{max} values spread across this range. In this paper, we present the sequences of two pigments isolated from Humbolt penguin and pigeon with intermediate λ_{max} values of 403 and 409 nm, respectively. By comparing the amino acid sequences of these pigments with the true UV pigments of budgerigar and canary and with chicken violet with a λ_{max} value of 420 nm, we have been able to identify five amino acid sites that show a pattern of substitution between species that is consistent with differences in λ_{max}. Each of these substitutions has been introduced into budgerigar cDNA and expressed in vitro in COS-7 cells. Only three resulted in spectral shifts in the regenerated pigment; two had relatively small effects and may account for the spectral shifts between penguin, pigeon, and chicken whereas one, the replacement of Ser by Cys at site 90 in the UV pigments, produced a 35 nm shortwave shift that could account for the spectral shift from 403 nm in penguin to around 370 nm in budgerigar and canary.

Visual pigments are members of the superfamily of G protein coupled receptors which function through the activation of a guanine nucleotide binding protein (G protein) and an effector enzyme which changes the levels of a second messenger in the cell cytoplasm. In vertebrates, a single rod and up to four cone classes of visual pigments may be present, classified as longwave (LW) with a peak of maximal absorbance (λ_{max}) of 530−570 nm, middlewave (MW) with λ_{max} of 480−520 nm, shortwave (SW) with λ_{max} of 440−460 nm, and violet/ultraviolet (V/UV) with λ_{max} lying between 430 and 355 nm. In mammals, however, this complement is reduced to only two classes, LW and V/UV, with a recent duplication of the LW class in Old World primates (*1*) and the New World Howler monkey (*2, 3*) responsible for the so-called "red" and "green" pigments.

Visual pigments are based on a common basic structure of an opsin protein covalently attached via a Schiff base linkage to a chromophore. The opsin part of the visual pigment in vertebrates consists of a single polypeptide chain of 340−370 amino acids that forms 7 α-helical transmembrane (TM) regions connected by cytoplasmic and extracellular loops (*4, 5*). In the tertiary structure, the seven α-helices form a bundle within the membrane, creating a cavity on the extracellular side for the chromophore, 11-*cis*-retinal, which is covalently bound to a conserved lysine residue in TM helix VII via a Schiff base linkage. The interaction of the chromophore with the opsin protein has been extensively studied in bovine rhodopsin. In this pigment, the Schiff base linkage is protonated, and the positive charge on the nitrogen is stabilized in the ground state by a counterion provided by an ionized glutamate residue at position 113 on the luminal end of TM helix III (*6*). Glutamate is found at the equivalent position in all other vertebrate opsins sequenced so far, with the exception of *Xenopus* violet opsin (*7*) where an aspartate residue is present and presumably serves the same purpose.

Each visual pigment shows a characteristic λ_{max}; the precise location of this peak in the spectrum depends on interactions between the chromophore and the opsin protein. Site-directed mutagenesis of bovine rod opsin (*8, 9*) and human red and green cone opsins (*10, 11*) has identified a number of tuning sites within the molecule which, when substituted, result in spectral shifts between pigments. With the exception of the chloride ion-binding site provided by amino acids 197 and 200 in the luminal loop connecting helices III and IV of primate red and green pigments and responsible for a 10−15 nm spectral shift (*12*), these sites are located in the TM regions of the molecule. A model based on conserved residues across approximately 500 G protein linked receptor proteins (*13, 14*), and refined by crystallographic studies (*15*−*17*), provides a framework for orientating each helix with respect to the exterior lipid membrane and the central hydrophilic pocket. Only changes in residues that either line this pocket or face another helix appear to have major effects on the spectral tuning of the resulting pigments (*18*). The particular λ_{max} of a visual pigment is thought to depend on

[†] This work was supported by project grants from the Biotechnology and Biological Sciences Research Council, U.K. and the National Science Foundation.

* To whom correspondence should be addressed.
[‡] Department of Molecular Genetics, University College London.
[§] Department of Biological Sciences, University of Maryland Baltimore County.
[||] Department of Visual Science, University College London.

10.1021/bi992776m CCC: $19.00
Published on Web 06/14/2000

at least two factors. First, the strength of the electrostatic interaction between the Glu113 counterion and the protonated Schiff base is critical, with an increase in the strength of the interaction resulting in a SW shift due to stabilization of the ground state (*19, 20*). Second, photoexcitation of 11-*cis*-retinal induces a significant increase in π electron delocalization and a corresponding change in dipole moment with a shift of net positive charge toward the β-ionone ring (*21, 22*). Interactions with charged, polar, or polarizable residues that alter delocalization will lead to a change in the energy difference between ground and excited states. An increase in delocalization will result in a LW shift in the absorbance spectrum and a decrease to a SW shift.

The V/UV class of opsins shows some of the largest naturally occurring variations in λ_{max}, ranging, for example, in mammals from around 430 nm in primates (*23*) to less than 370 nm in rodents (*24*), and in birds from around 420 nm in chicken (*25*) and duck (*26*) to around 365 nm in canary (*27*) and budgerigar (*28*).

Some progress in understanding the mechanism of tuning of this class of pigments has recently been made (*29*) using sequence comparisons between human rod and violet (blue) cone opsins. By replacing the amino acids present in human rod with those in the human violet opsin, six sites were identified that together may account for about 80% of the spectral shift from 500 nm of human rod to around 425 nm of human violet pigment. A subsequent study (*30*) has however emphasized the inherent problems of substituting across different classes of opsins. Starting with human violet opsin, the reverse mutations of amino acids in the vicinity of the β-ionone ring produced the expected shifts whereas those near the Schiff base did not.

We have taken advantage of the natural variation in λ_{max} values of avian V/UV pigments, thus avoiding the problems of substituting between different classes of opsins, and we have concentrated on shifts from 420 nm into the ultraviolet. In addition to the chicken (*31*), budgerigar (*28*), and canary (*27*) pigments where the gene sequences have already been reported, we have sequenced UV/V opsin cDNAs from the pigeon, *Columba livia* (*32*), with a λ_{max} around 409 nm, and from the Humbolt penguin, *Spheniscus humboldti* (*33*), with a λ_{max} around 403 nm. These latter two species provide therefore pigments with λ_{max} values that are somewhat intermediate between the violet and true UV pigments. By comparing these sequences, we have been able to identify candidate sites for spectral tuning in the ultraviolet region of the spectrum. The effects of these sites on tuning have been examined in the budgerigar UV−visual pigment by site-directed mutagenesis, in vitro expression, and regeneration of recombinant pigments. From this, we have been able to identify a set of three substitutions that together can account for the major part of the spectral difference between chicken violet and budgerigar/canary UV pigments, a shift of around 45 nm.

EXPERIMENTAL PROCEDURES

cDNA Cloning and Sequencing. mRNA was extracted from the retinas of recently sacrificed pigeons and from previously frozen eyes from Humboldt penguin; the former were obtained from commercial sources while the latter came from zoo animals which had been sacrificed for humane reasons. A Pharmacia Quickprep Micro mRNA purification kit was used for the purpose. Single-stranded cDNA was synthesized using an oligo-dT primer and used as template in PCRs using degenerate oligonucleotide primers designed from known avian violet/UV opsin sequences. In this way, partial V/UV opsin cDNA sequences from the indicated species were amplified comprising the sequences for all seven α-helical regions. The sequences (IUB codes) of the forward and reverse primers used were, respectively, 5′-CCCVYTSAACGCCRTSGT-3′ (v141+) and 5′-TGGCTG-GWGGASACRGAGGA-3′ (v1040−). These partial opsin sequences were inserted into the pGEM-T Easy vector system II (Promega) and fully sequenced. The sequences were identified as presumptive violet/UV opsin sequences on the basis of nucleotide and amino acid similarity with chicken violet (*31*) and budgerigar UV (*28*) opsin sequences. To eliminate the possibility of errors being introduced during the PCRs, cloned fragments from three independent PCRs were sequenced throughout.

In the case of the pigeon violet opsin, the complete cDNA sequence was obtained using a 5′/3′-RACE and the following sequence specific primers: 5′-GGCCTCCAAGGCACA-CATGTC-3′ (Pv336−) and 5′-CGACCTGCGCCTCGT-CACCA-′ (Pv833+).

Construction of Budgerigar UV Opsin Expression Vector and Generation of Violet/UV Opsin Mutants. Wild-type budgerigar UV opsin was amplified from budgerigar retinal cDNA with *Pfu* DNA polymerase using the following forward and reverse primers: BUV5+, 5′-GCGCGAAT-TCCACCATGTCGGGTGAGGAGGAGTTTTAC-3′; and BUV3−, 5′-CGGCGTCGACGCGCTGGGGCTGACCTG-GCTGGA-3′. The resulting fragment containing the entire budgerigar UV coding sequence was then directionally transferred as the *Eco*RI *Sal*I fragment into a derivative of the mammalian expression vector pMT2 carrying the sequence of the bovine rhodopsin 1D4 epitope (including the stop codon) downstream and in-frame with the *Sal*I site (*34*). The sequence of the resulting opsin fragment was then checked using budgerigar UV opsin sequencing primers.

The above budgerigar UV *Eco*RI *Sal*I fragment was then inserted into the vector pALTER-1 for generation of site-directed mutations using the Promega Altered Sites system. Mutations were introduced into the budgerigar UV opsin sequence at five candidate tuning sites in which the codon for the amino acid present in the budgerigar UV sequence was substituted by the codon for the amino acid present in the chicken violet sequence. The oligonucleotides used for the mutagenesis were as follows: A81S, 5′-GTGGGTTC-CTCTCCTGTATCATC-3′; C85S, 5′-CCTGTATCATCAG-CATCTTCACC-3′; T88V, 5′-CATCTGCATCTTCGT-CGT-CTTCGTC-3′; A113T, 5′-GGCTTCATGGGTACCACTG-CAGGG-3′; S293A, 5′-CTCCAAGAGCGCCTGCGTCTAC-3′.

The numbering of amino acid residues corresponds to the budgerigar UV opsin. The nucleotides underlined represent the mutagenic substitutions. Following mutagenesis, the nucleotide sequence of the entire opsin fragment was confirmed, and the *Eco*RI *Sal*I fragment was reinserted into the expression vector.

Expression, Purification, and Characterization of Wild-Type Budgerigar UV and Mutant Pigments. Clones were

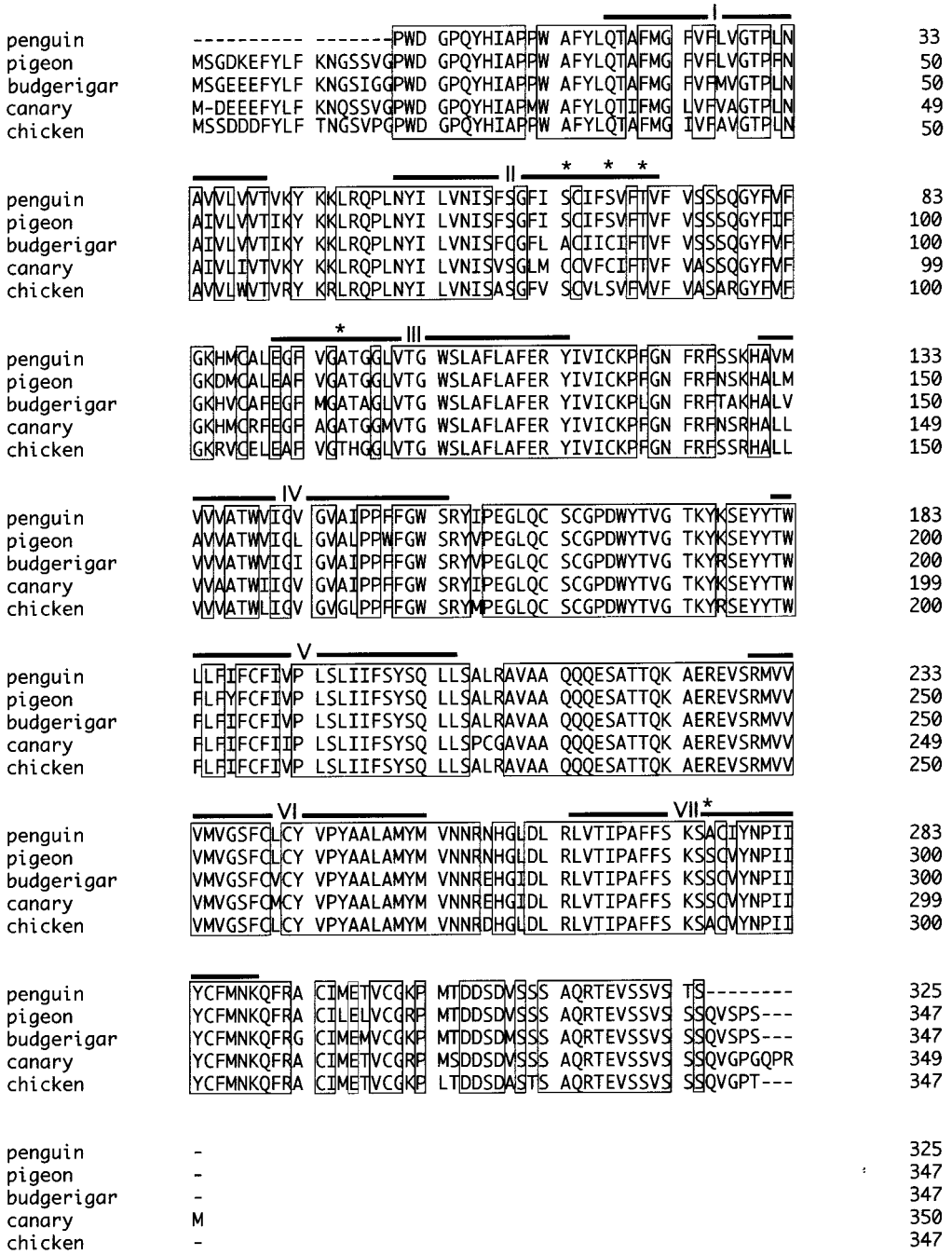

FIGURE 1: Deduced amino acid sequences of the violet opsins from pigeon (accession no. AJ238856) and penguin aligned with the chicken violet opsin (*31*) and UV opsins from the canary (*27)* and budgerigar (*28*). The position of each of the seven α-helical transmembrane regions is indicated by a horizontal line. The five candidate sites investigated in this work are starred.

transiently expressed in COS-7 cells following transfection with lipofectamine (Gibco-BRL). Cells were harvested 48 h post-transfection. Pigment was generated by suspending the cells in PBS and incubating with 40 μM 11-*cis*-retinal in the dark (*35*, *36*). Pigment was solubilized from cell membranes as described (*37*) and was purified by immunoaffinity chromatography using a monoclonal antibody directed against the 1D4 epitope of bovine rhodopsin (*36*).

Purified pigments eluted from the immunoaffinity matrix were maintained at 14 °C in a water-jacketed cuvette holder. Absorption spectra were recorded in the dark using a Hitachi model U-3300 dual-path spectrophotometer. Acid denaturation spectra were recorded after addition of 1 N HCl to bring the pH to less than 2.

Determination of λ_{max} of Expressed Pigments. Where possible, the λ_{max} values of expressed pigments were determined by the direct fitting of a standard rhodopsin A_1 template (*38*) to the experimental data. Where this was not possible, the λ_{max} values were derived from the difference spectrum of the neutral (pH 7.2) minus the acid denaturation (pH <2) spectra. As is commonly observed when solubilizing expressed pigments, the direct absorption spectra had a baseline slope that increased with decreasing wavelength (Figure 2), due to nonspecific absorption or to scattering by cellular debris or other material. Acidification reduced the extent of this baseline slope, probably due to solubilization of some of the material producing the scattering. Consequently, all difference spectra had a corresponding baseline

slope which required flattening for accurate spectral analysis.

A series of difference spectra were generated from the standard templates of rhodopsin A_1 (*38*) and acid-denatured bovine rhodopsin (*39*) by (i) varying the λ_{max} of the rhodopsin A_1 template at 1 nm intervals from 350 to 400 nm and (ii) adjusting the ratio of the peak absorbance of the acid-denatured rhodopsin template to that of the native rhodopsin template in increments of 0.05 in the range 0.25−1.8. These were then fitted to the experimental data. The nonlinear baseline slope was well described by a simple quadratic function, and this was used to remove it as follows. However, because acidification produces a very clear spectral shift, the analysis of the difference spectra was relatively insensitive to the function used to flatten the baseline. The isosbestic point for each template pair (defined as the point at which the shortwave arm of the rhodopsin template crossed the spectrum of the acid-denatured bovine rhodopsin template) was noted; it was typically located about 20 nm below the rhodopsin λ_{max} (with some variation depending on the peak absorption ratio). Assuming that the difference spectra of the experimental data showed an actual absorbance change of zero at this isosbestic point, each spectrum was corrected from this point through to 600 nm by subtracting a baseline calculated as follows:

$$\text{baseline} = \alpha(600 - \lambda)^2$$

where α is the absorbance of the experimental data at the isosbestic point (A_{IP}) divided by $(A_{600} - A_{IP})^2$.

This correction was applied as each test difference spectrum was tested for fit, and the goodness of fit was then computed as the sum of squares of differences between the computed template and the corrected data (from 340 to 500 nm). The λ_{max} value of the rhodopsin template component of the difference spectrum giving the best fit (minimum sum of squares of deviations) was taken as the λ_{max} of the expressed pigment.

RESULTS

Selection of Amino Acid Residues for Substitution. The deduced amino acid sequences for the penguin and pigeon opsin sequences, aligned with budgerigar (*28*) and canary UV (*27*) and chicken violet (*31*) opsins, are shown in Figure 1. The three-dimensional model of G protein coupled receptors (*13, 14*) was used to identify the seven transmembrane helices for each opsin. Candidate tuning sites were identified within these helices where nonconservative amino acid substitutions occurred between opsins from species with differing λ_{max} values, at positions on the helices likely to point into the retinal binding cavity (*13, 14*). This approach yielded five candidate tuning sites as follows: A81S, C85S, T88V, A113T, and S293A in budgerigar UV and chicken violet, respectively (Table 1). On the bovine rod opsin numbering system, these are equivalent to positions 86, 90, 93, 118, and 298. For reasons of comparability, the bovine numbering system will be used hereafter.

Spectral Properties of Wild-Type and Mutant Opsins. Mutations were generated at each of the five sites by site-directed mutagenesis of budgerigar UV opsin. In each case, changes resulted in the substitution of the amino acid present in chicken violet opsin as follows: A86S, C90S, T93V, A118T, and S298A. The mutant opsin cDNAs as well as the wild-type budgerigar UV cDNA were transiently expressed in COS-7 cells, reconstituted with 11-*cis*-retinal, and the proteins were purified as described previously.

Table 1: Candidate Spectral Tuning Sites for Avian UV/Violet Pigments

		amino acid sites[b]				
species	λ_{max} (nm)[a]	86	90	93	118	298
canary	366	C	C	T	A	S
budgerigar	371 (365)	A	C	T	A	S
pigeon	409 (393)	S	S	T	A	S
penguin	403	S	S	T	A	A
chicken	418	S	S	V	T	A

[a] λ_{max} values were obtained from in vivo measurements by microspectrophotometry (*25, 27, 29, 33*). Values in parentheses were obtained from in vitro expressed and regenerated pigments (*24, 28*). [b] Bovine rod numbering.

The wild-type budgerigar UV pigment produced in this expression system produced an absorbance spectrum (Figure 2a) which gave a good fit to a standard rhodopsin template (*38*) with an estimated λ_{max} of 363 nm (Figure 3a). This λ_{max} value is in close agreement with the λ_{max} value of 365 ± 3 nm obtained for the corresponding His-tagged protein expressed in the recombinant baculovirus system (*28*). It is, however, slightly shorter than the in situ value of 371 ± 5 nm measured by microspectrophotometry (*40*). It was observed that the spectra produced from both the wild-type recombinant pigment and the mutant pigments gave a closer fit to the standard rhodopsin template (*38*) than to the modified UV pigment template derived from *Danio* and other species (*41*), which has a slightly narrower absorption bandwidth than the former. The broader bandwidth and the slightly shorter λ_{max} value measured for the recombinant pigment compared to the native pigment may indicate slight structural changes in the pigment when present in detergent solution rather than in cone cell membranes.

All five of the mutants produced absorbance spectra indicative of photosensitive pigments (Figure 2b−f). However, with the exception of the S298A mutant, the spectra of the mutants suffered from light scattering in the UV region, and the sizes of the chromophore peak (α peak) were noticeably smaller than that obtained for the wild-type pigment, presumably as a result of protein instability or less efficient chromophore binding, such that they appeared as shoulders on the main protein peak (γ peak). As a result, only the spectrum from mutant S298A could be analyzed by simple rhodopsin template fitting, and an alternative approach was used for the other spectra.

Acidification of a photopigment to a pH of 1.9 results in denaturation of the protein and the generation of a simple protonated Schiff base of 11-*cis*-retinal, which gives a spectral absorbance of around 440 nm. All five mutants as well as the wild-type pigment produced the expected shifts in λ_{max} on acid denaturation, thus confirming the Schiff base linkage between opsin and chromophore. As detailed under Experimental Procedures, the λ_{max} values for the neutral pigment (pH 7.2) of the A86S, C90S, T93V, and A118T mutants were derived in each case from the difference spectrum of the neutral minus the acid denaturation (pH <2) spectra. A series of theoretical difference spectrum templates were then generated from the standard rhodopsin template (*38*) and a standard acid denaturation spectrum for bovine

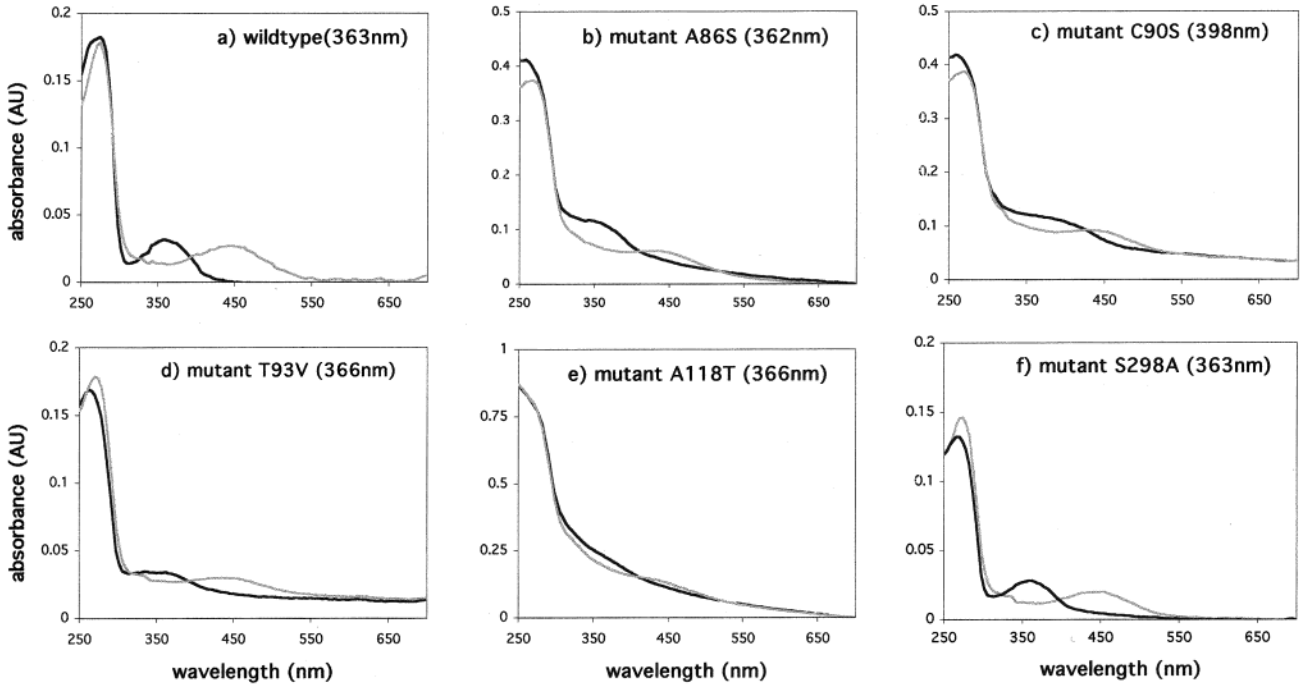

FIGURE 2: Absorbance spectra of purified budgerigar UV pigment and point mutants expressed in COS-7 cells. Direct spectra of (a) wild type, (b) mutant A86S, (c) mutant C90S, (d) mutant T93V, (e) mutant A118T, and (f) mutant S298A pigments, recorded at pH 7.2 (black line) and after acidification to pH 1.9 with 1 N HCl (gray line). λ_{max} values for the pigments derived from these spectra are given in parentheses.

rhodopsin (*39*) and fitted to the experimental difference spectrum. The spectral location of the standard rhodopsin template of the best-fit template difference spectrum allowed an estimate of λ_{max} of the neutral pigment. The analysis for mutant C90S is shown in Figure 3b. λ_{max} values estimated for the wild-type pigment and for mutant S298A using this method agreed with values obtained by fitting a rhodopsin template directly to the dark spectrum to an accuracy of ± 1 nm.

The λ_{max} values measured for budgerigar UV pigment and the five mutant pigments are given in Table 2. The pigment with the C90S substitution shows a substantial 35 nm red shift. Mutants T93V and A118T showed much smaller shifts of approximately 3 nm, mutant A86S produced a 1 nm shift but in the opposite direction, and mutant S298A was without effect. The latter two sites can be discounted, therefore, as important for spectral tuning. The small spectral shifts arising from the T93V and A118T mutants are more difficult to assess, although the relatively good fit of the experimental data for T93V (Figure 2d) to the test templates suggests that in this case, at least, there is a small but real change in spectral position.

Location of Tuning Sites within the Chromophore Binding Pocket. A model for the α-carbon positions of the seven α-helical TM regions of rhodopsin has been proposed by Baldwin et al. (*13, 14*). This model utilizes sequence data from around 500 members of this G protein coupled receptor family and the density of the three-dimensional map of frog rhodopsin determined by electron cryo-microscopy (*15, 16*). In this model, helices I, II, III, and V are tilted with respect to the other three helices, thereby placing the counterion residue at position 113 at the base of helix III in close proximity to the protonated Schiff base. The chromophore is contained within the pocket formed by the helices, with the β-ionone ring of the chromophore adjacent to helices III

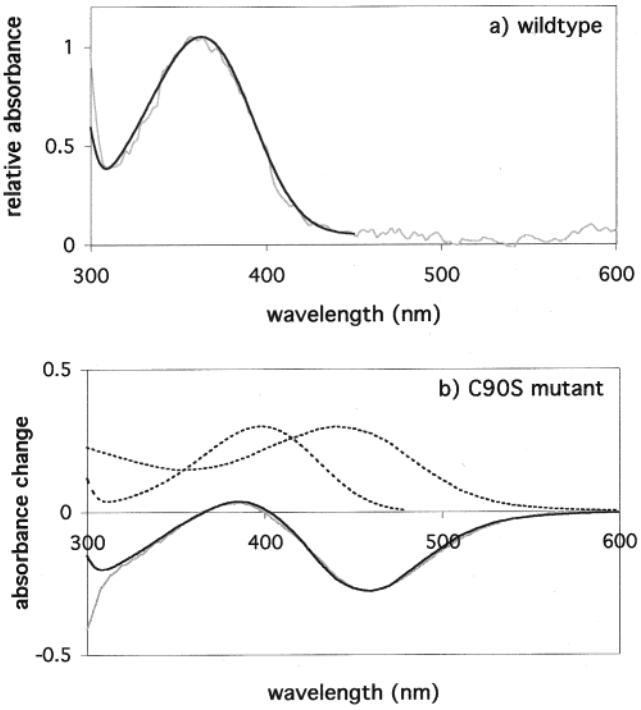

FIGURE 3: Derivation of λ_{max} values for the pigments from the raw spectra. (a) Fitting of a standard rhodopsin template (black line) (*38*) to experimental data (gray line) for wild-type pigment; estimated $\lambda_{max} = 363$ nm. (b) Estimation of λ_{max} value for mutant C90S from analysis of the difference spectrum (spectrum at pH 7.2 minus spectrum at pH 1.9). The experimental difference spectrum (gray line) is shown fitted to the best difference template (standard rhodopsin template minus standard acid denaturation template)(black line). The standard rhodopsin template (*38*) and acid denaturation template (*39*) from which the difference template is derived are shown (dotted lines). The λ_{max} value derived for mutant C90S was 398 nm.

Table 2: Spectral Shifts Measured for Wild-Type Budgerigar UV Pigment and Site-Directed Mutants Expressed in COS-7 Cells

mutation	λ_{max} (nm)	shift from wild-type pigment[a] (nm)	Σd^2
wt	363	−	0.40
A86S	362	−1	1.74
C90S	398	+35	0.97
T93V	366	+3	0.30
A118T	366	+3	1.76
S298A	363	0	1.20

[a] λ_{max} shifts from budgerigar wt pigment are expressed as positive for red shifts and negative for UV shift. The goodness of fit of the template difference spectra to the experimental difference spectra is indicated by the sum of squares of deviations, Σd^2.

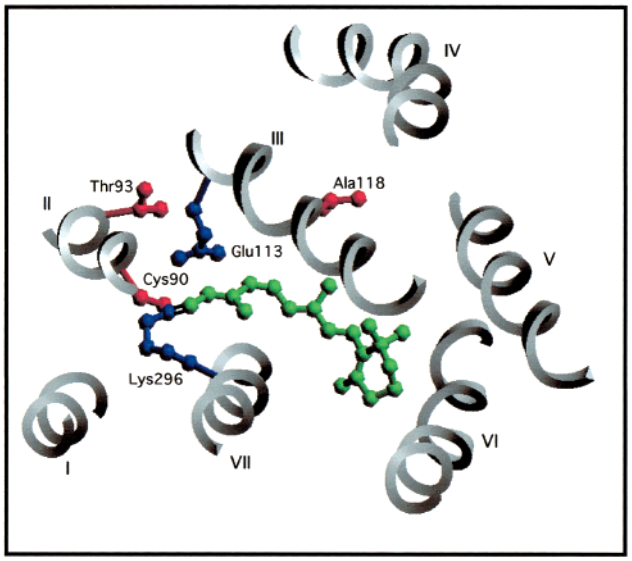

FIGURE 4: Structural model of the budgerigar UV pigment viewed from the cytoplasmic side of the membrane and showing part of each TM. The 11-*cis*-retinal chromophore is shown in green, and Lys296 and the counterion Glu113 are shown in blue. The three residues Cys90, Thr93, and Ala118, shown in this study to be involved in spectral tuning into the UV, are shown in red. The proximity of the sulfur atom of Cys90 to the Schiff base linkage is clearly seen. The model was built in Setor and is based on the theoretical model for bovine rhodopsin (*45*).

and VI (*42*), with the tilt of helix III accommodating an interaction also with the C9 methyl group of the polyene chain (*43*). Since the separation of the positive charge of the protonated Schiff base from its negative counterion is the immediate effect of the photoisomerization of retinal around the C_{11}═C_{12} bond, it follows that the strengthening or weakening of this interaction will lead respectively to a SW or LW shift in the λ_{max} of the pigment.

The relative positions of residues 90, 93, and 118, the Schiff base, and the Glu113 counterion are shown in a model of the avian UV pigment (Figure 4) generated from a theoretical model of bovine rhodopsin (*45*). It is of course not possible to say how accurately this model reflects the true structure of the avian UV pigment. In the model, residues 90 and 93 are located on the luminal side of helix II, at about the level of the counterion residue in helix III, whereas residue 118 is located just under two turns of helix III above site 113 and lies alongside the polyene chain of the chromophore. The major shift is achieved by the C90S substitution, which involves the simple replacement of an SH with an OH group on the side chain. In contrast, the much smaller longwave shift associated with the T93V substitution involves the loss of a polar group in the region of the counterion. Substitutions adjacent to the polyene chain of the chromophore most likely interact electrostatically to modify the charge distribution in the ground and excited states and thereby shift the absorption maximum (*29*). The third tuning site at position 118 occupies such a location, and the A118T substitution may be expected to have its effect on λ_{max} by this mechanism.

DISCUSSION

A comparison of the deduced amino acid sequences of five avian opsins in the V/UV class has enabled us to identify five candidate sites for spectral tuning in the violet and UV regions of the spectrum. When the amino acid residues present at these five sites in the longer-wave-sensitive chicken violet opsin were substituted in the budgerigar UV opsin, only substitutions at sites 90, 93, and 118 generated LW spectral shifts. The largest shift was achieved by a C90S substitution. This substitution distinguishes the two true UV-sensitive pigments of budgerigar and canary from the violet-sensitive pigments of the pigeon, penguin, and chicken. Moreover, if the microspectrophotometric measurements of λ_{max} are used (and taking into account the error limits of the measurements), the spectral shift of 35 nm achieved by this substitution effectively accounts for the difference between the budgerigar UV pigment at 371 nm and the penguin and pigeon violet pigments at 403 and 409 nm, respectively. The other two tuning sites are substituted only in chicken violet opsin; assuming that their effects are additive, they could together produce a further LW shift of 6 nm and thus account for much of the shift to 418 nm in chicken violet pigment.

Our results indicate that SW tuning involves the gain of polar groups in the vicinity of the protonated Schiff base and the loss of polar groups adjacent to the polyene chain and β-ionone ring, consistent with the results of previous workers (*10*, *11*, *29*, *44*). Tuning sites 90 and 93 are both in the vicinity of the protonated Schiff base; the V93T substitution introduces an additional polar hydroxyl group whereas the S90C substitution exchanges a hydroxyl for a thiol group. This latter change does not amount to a substantial change in polarity. The major difference between a thiol and a hydroxyl group is that the thiol is more ionizable; the UV shift may result, therefore, from a pK_a effect. The local environment of C90 may serve to reduce its pK_a such that a thiolate ion is present under neutral conditions. Such an anion, together with the increased polarity provided by T93, could further stabilize the proton on the Schiff base in the ground state of the pigment, with a consequent spectral shift into the UV. As shown in the model of avian UV pigment depicted in Figure 4, the close proximity of C90 to both the Schiff base linkage and the counterion of E113 lends support to this hypothesis. Site 118, on the other hand, lies toward the luminal side of helix III and is adjacent to the polyene chain of the chromophore. The T118A substitution results in the loss of a polar hydroxyl group in the SW-shifted pigments. In this case, the effect may be to destabilize the excited state of the chromophore due to a reduced ability to stabilize the positive charge of the β-ionone ring generated on photoexcitation.

The S90C substitution appears, therefore, to be the most important change for pigment tuning into the UV in birds.

All the other vertebrate UV opsins sequenced to date, from the mouse (*46*), rat (*47*), Anolis lizard (*48*, *49*), and goldfish (*50*), retain S90. It follows from this that an alternate mechanism must be involved in spectral shifts into the UV in nonavian species.

ACKNOWLEDGMENT

We thank Professor Martin Warren for helpful discussions on the interpretation of our data, Dr. Rosalie Crouch for the generous provision of a sample of 11-*cis*-retinal, and Chester Zoo, U.K., for the penguin tissue.

REFERENCES

1. Ibbotson, R. E., Hunt, D. M., Bowmaker, J. K., and Mollon, J. D. (1992) *Proc. R. Soc. London, Ser. B B247*, 145−154.
2. Jacobs, G. H., Neitz, M., Deegan, J. F., and Neitz, J. (1996) *Nature 382*, 156−158.
3. Hunt, D. M., Dulai, K. S., Cowing, J. A., Julliot, C., Mollon, J. D., Bowmaker, J. K., Li, W.-H., and Hewett-Emmett, D. (1998) *Vision Res. 38*, 3299−3306.
4. Dratz, E., and Hargrave, O. (1983) *Trends Biochem. Sci. 8*, 128−133.
5. Findlay, J. B. C., and Pappin, D. J. C. (1986) *Biochem. J. 238*, 625−642.
6. Sakmar, T. P., Franke, R. R., and Khorana, H. G. (1989) *Proc. Natl. Acad. Sci. U.S.A. 86*, 8309−8313.
7. Starace, D. M., and Knox, B. E. (1998) *Exp. Eye Res. 67*, 209−220.
8. Nathans, J. (1990) *Biochemistry 29*, 937−942.
9. Nakayama, T. A., and Khorana, H. G. (1991) *J. Biol. Chem. 266*, 4269−4275.
10. Merbs, S. L., and Nathans, J. (1993) *Photochem. Photobiol. 58*, 706−710.
11. Asenjo, A. B., Rim, J., and Oprian, D. D. (1994) *Neuron 12*, 1131−1138.
12. Wang, Z., Asenjo, A., and Oprian, D. D. (1993) *Biochemistry 32*, 2125−2130.
13. Baldwin, J. M. (1993) *EMBO J. 12*, 1693−1703.
14. Baldwin, J. M., Schertler, G. F. X., and Unger, V. M. (1997) *J. Mol. Biol. 272*, 144−164.
15. Schertler, G. F. X., Villa, C., and Henderson, R. (1993) *Nature 362*, 770−772.
16. Schertler, G. F. X., and Hargrave, P. A. (1995) *Proc. Natl. Acad. Sci. U.S.A. 92*, 11578−11582.
17. Unger, V. M., Hargrave, P. A., Baldwin, J. M., and Schertler, G. F.(1997) *Nature 389*, 203−206.
18. Hunt, D. M., Fitzgibbon, J., Slobodyanyuk, S., and Bowmaker, J. K. (1996) *Vision Res. 36*, 1217−1224.
19. Blatz, P. E., Mohler, J. H., and Navangul, H. V. (1972) *Biochemistry 11*, 848−855.
20. Kakitani, H., Kakitani, T., Rodman, H., and Honig, B. (1985) *Photochem. Photobiol. 41*, 471−479.
21. Kropf, A., and Hubbard, R. (1958) *Ann. N.Y. Acad. Sci. 74*, 266−280.
22. Mathies, R., and Stryer, L. (1976) *Proc. Natl. Acad. Sci. U.S.A. 73*, 2169−2173.
23. Bowmaker, J. K., Astell, S., Hunt, D. M., and Mollon, J. D. (1991) *J. Exp. Biol. 156*, 1−19.
24. Yokoyama, S., Radlwimmer, F. B., and Kawamura, S. (1998) *FEBS Lett. 423*, 155−158.
25. Maier, E. J., and Bowmaker, J. K. (1993) *J. Comput. Physiol. A172*, 295−301.
26. Jane, S. D., and Bowmaker, J. K. (1988) *J. Comput. Physiol. A165*, 225−235.
27. Das, D., Wilkie, S. E., Hunt, D. M., and Bowmaker, J. K. (1999) *Vision Res. 39*, 2801−2815.
28. Wilkie, S. E., Vissers, M. A. M., Das, D., DeGrip, W. J., Bowmaker, J. K., and Hunt, D. M. (1998) *Biochem. J. 330*, 541−547.
29. Lin, S. W., Kochendoerfer, G. G., Carroll, K. S., Wang, D., Mathies, R. A., and Sakmar, T. P. (1998) *J. Biol. Chem. 273*, 24583−24591.
30. Fasick, J. I., Lee, N., and Oprian, D. D. (1999) *Biochemistry 38*, 11593−11596.
31. Okano, T., Kojima, D., Fukada, Y., Shichida, T. Y., and Yoshizawa T. (1992) *Proc. Natl. Acad. Sci. U.S.A. 89*, 5932−5936.
32. Wilkie, S. E., Bowmaker, J. K., and Hunt, D. M. (1998) *Invest. Ophthalmol. Visual Sci. 39*, S957.
33. Bowmaker, J. K., and Martin, G. R. (1985) *J. Comput. Physiol. A156*, 71−77.
34. Franke, R. R., Sakmar, T. P., Oprian, D. D., and Khorana, H. G. (1988) *J. Biol. Chem. 263*, 2119−2122.
35. Oprian, D. D., Molday, R. S., Kaufman, R. J., and Khorana G. H. (1987) *Proc. Natl. Acad. Sci. U.S.A. 84*, 8874−8878.
36. Molday, R. S., and MacKenzie, D. (1983) *Biochemistry 22*, 653−660.
37. Okano, T., Fukada, Y., Artamonov, I. D., and Yoshizawa, T. (1989) *Biochemistry 28*, 8848−8856.
38. Stavenga, D. A., Smits, R. P., and Hoenders, B. J. (1993) *Vision Res. 33*, 1011−1017.
39. Knowles, A., and Dartnell, H. J. A. (1977) in *Photobiology of Vision, 2B, The Eye* (Davson, H., Ed.) pp 1−689, Academic Press, New York.
40. Bowmaker, J. K., Heath, L. A., Wilkie, S. E., and Hunt, D. M. (1997) *Vision Res. 37*, 2183−2194.
41. Palacios, A. G., Goldsmith, T. H., and Bernard, G. D. (1996) *Vis. Neurosci. 13*, 411−421.
42. Nakayama, T. A., and Khorana, H. G. (1990) *J. Biol. Chem. 265*, 15762−15769.
43. Han, M., Groesbeek, M., Sakmar, T. P., and Smith, S. O. (1997) *Proc. Natl. Acad. Sci. U.S.A. 94*, 13442−13447.
44. Kochendoerfer, G. G., Wang, Z., Oprian, D. D., and Mathies, R. A. (1997) *Biochemistry 36*, 6577−6587.
45. Pogozheva, I. D., Lomize, A. L., Mosberg, H. I. (1997) *Biophys. J. 72*, 1963−1985.
46. Chiu, M. I., Zack, D. J., Wang, Y., and Nathans, J. (1994) *Genomics 21*, 440−443.
47. Zhao, X., Haeseleer, F. J., Fariss, R. N., Huang, J., Baehr, W., Milam, A. H., and Palczewski, K. (1997) *Vis. Neurosci. 14*, 225−232.
48. Kawamura, S., and Yokoyama, S. (1996) *Vision Res. 36*, 2797−2804.
49. Kawamura, S., and Yokoyama, S. (1998) *Vision Res. 38*, 37−44.
50. Hisatomi, O., Satoh, T., Barthel, L. K., Stenkamp, D. L., Raymond, P. A., and Tokunaga, F. (1996) *Vision Res. 36*, 933−939.

BI992776M